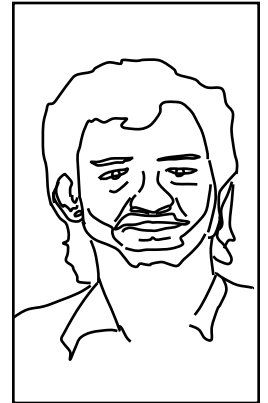
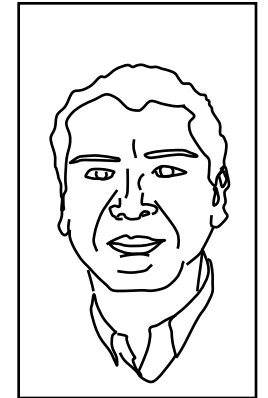


My 30-Year Collaboration with David



Boualem Hammouda
NIST Center for Neutron Research



A- SANS FROM POLYMERIC MATERIALS

B- SANS RESOLUTION AND NEUTRON FOCUSING

A- SANS FROM POLYMERIC MATERIALS

Collaboration with the Dow Chemical company

1. Hot stretching
2. Injection molding
3. Shear band formation under compression

1. Hot-Stretching

Macromolecular orientation affects mechanical properties.

Investigated macromolecular orientation associated with sample deformation and processing.

Used mixture of deuterated and non-deuterated polystyrene.

Samples were hot stretched in an Instron machine at various conditions.

SANS was used to measure the macromolecular orientation.

Elliptical averaging of SANS data.

Hot-Stretching

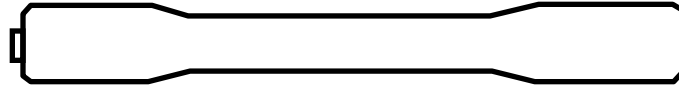


Table 1: Hot stretched bar samples and chain orientation results obtained from SANS and birefringence measurements

Sample	Load (lbs)	Stretch Rate (inch/min)	Temp (°C)	EDR	Eccent.	R _{gy} (Å)	R _{gx} (Å)	MDR	Birefring. *10 ³
CDS1	12.8	10	110	2.0	.45	249	112	1.70	5.74
CDS2	15.1	10	110	1.5	.75	170	127	1.21	1.78
CDS3	11	10	110	2.75	.33	293	97	2.09	8.80
CDS4	10	5	110	4	.30	330	99	2.23	10.02
CDS5	--	10	110	1.75	.54	214	116	1.51	4.21

Hot-Stretching

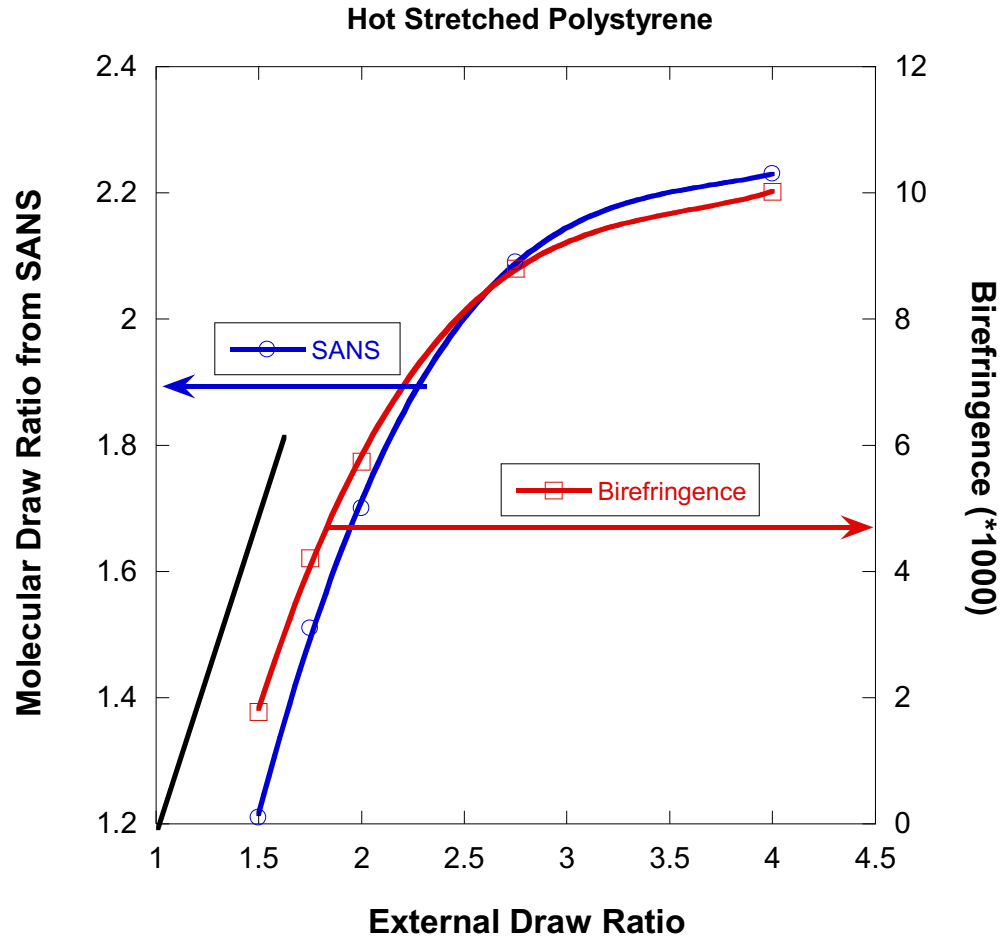


Figure 2: Plot of the **Molecular Draw Ratio** for varying **External Draw Ratio**. Results from SANS and **birefringence measurements** are included. The line with a slope of 1 is also shown.

Hot-Stretching

Hot Stretched Polystyrene

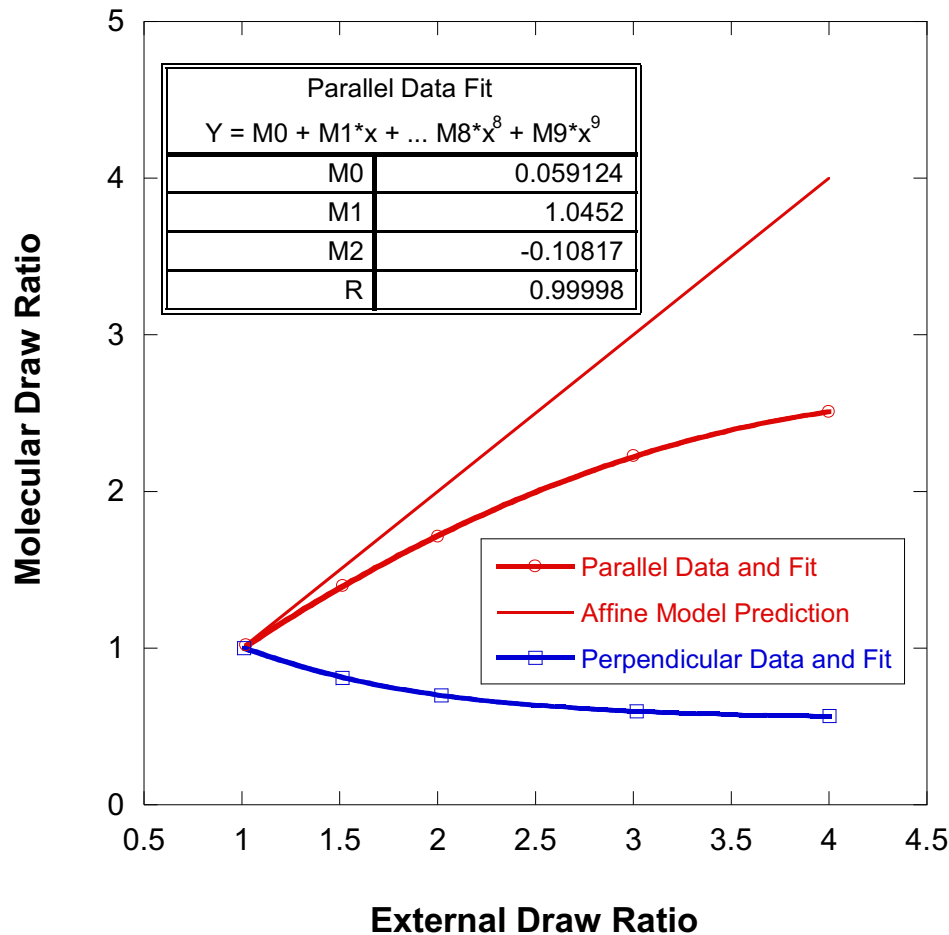


Figure 2: Plot of the **Molecular Draw Ratio** for varying **External Draw Ratio**. Deformations are **non affine**.

2. Injection Molding

Mixture of deuterated and non-deuterated polystyrene

Injection molding at **various conditions** and with **various shapes**

Table 2: Injection molding conditions

	Cold Conditions	Hot Conditions
Melt Temperature	167 °C	229 °C
Pressure	3700 psi	2500 psi
Injection Time	8 s	8 s
Cooling Time	30 s	30 s
Band Temperature	176 °C	246 °C
Mold Temperature	24 °C	65 °C

Injection Molding

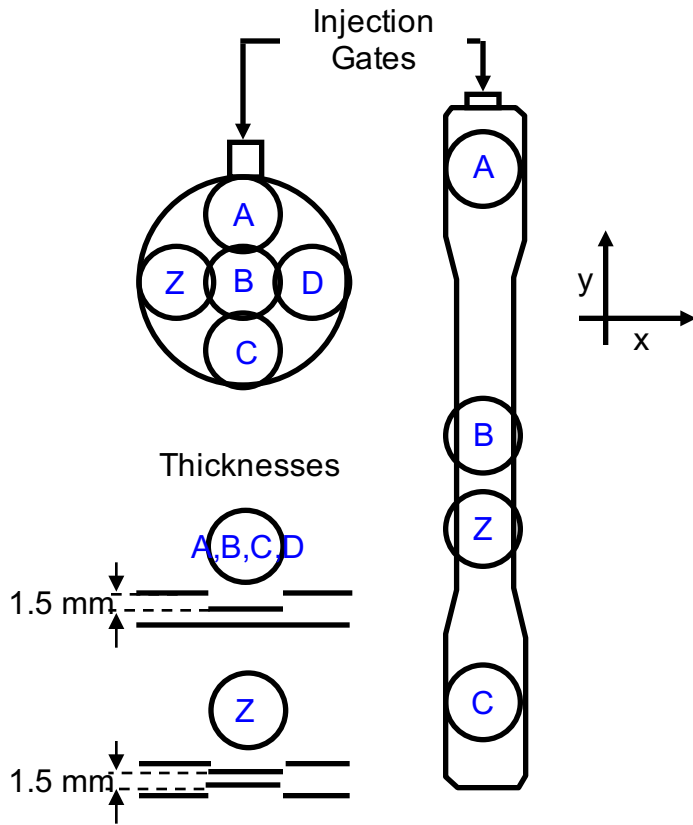
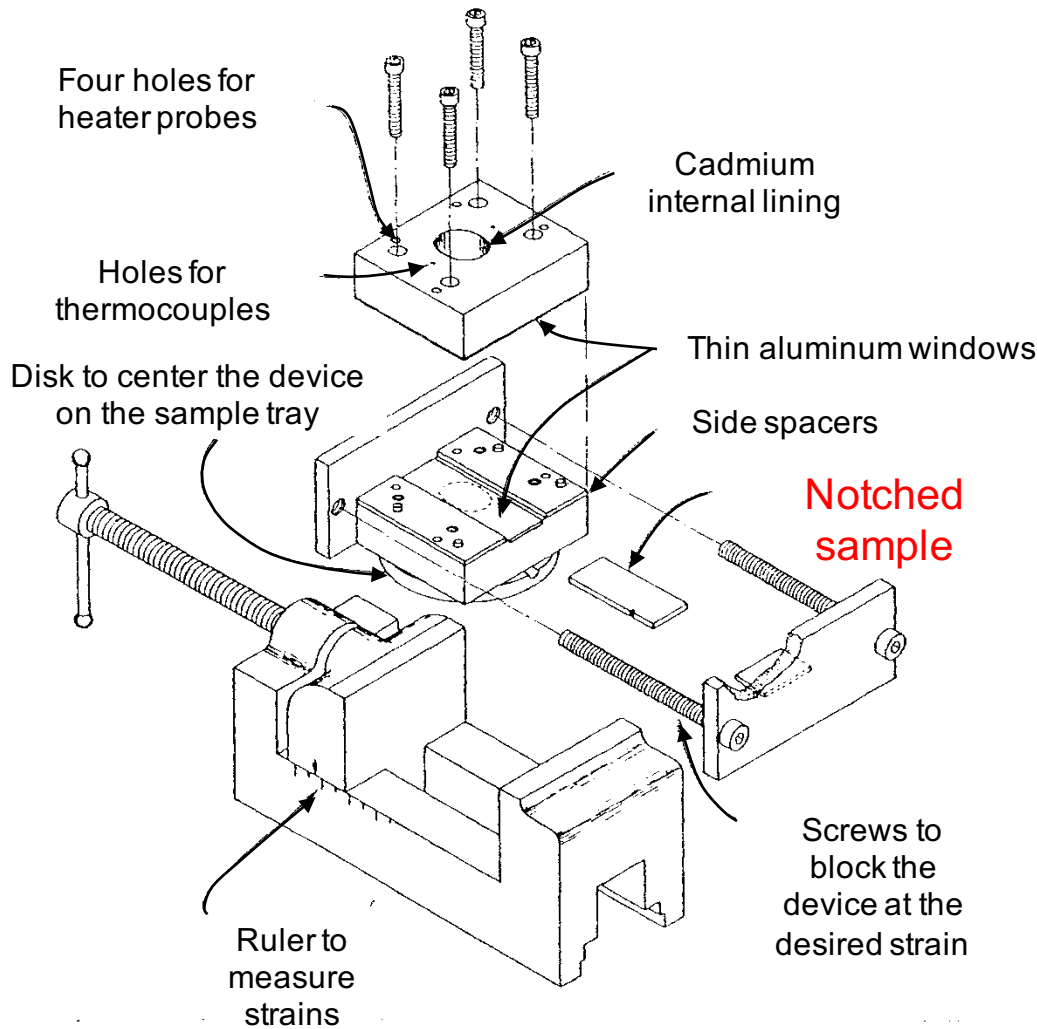


Table 3: **Eccentricity** and orientation angle for one of the injection molded samples (**cold molded disk**).

	Eccentricity	Orientation Angle (degrees)
Spot A	.63	5
Spot B	.77	9
Spot C	.87	24
Spot D	.79	38
Spot Z	.92	40

Figure 4: Injection molded disk and bar.

3. Shear Band Formation



Mixture of deuterated and non-deuterated polystyrene

Notched and compressed sample

Shear bands were formed by compression in a device

Various temperatures, strains and strain rates

Figure 5: Representation of the device used to create shear bands.

Shear Band Formation

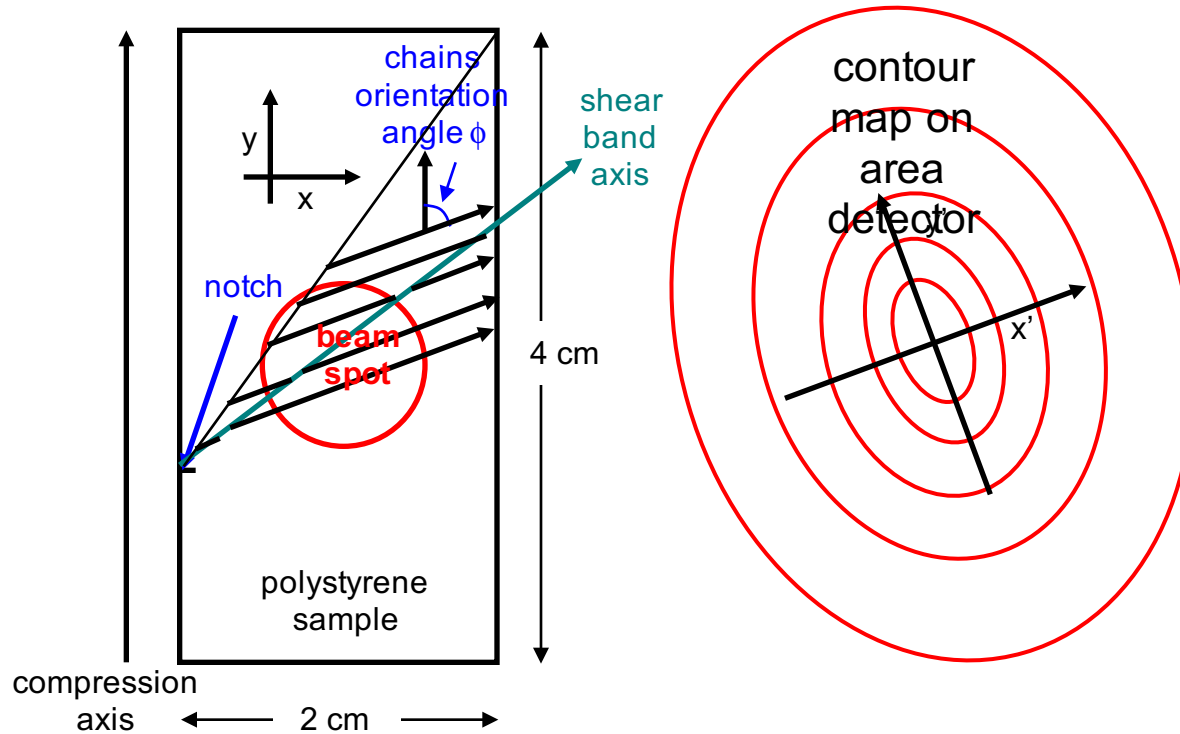


Figure 6: Representation of the **sample plane** (in direct space) and of the **scattering plane** (reciprocal space). Note that **the shear band axis** and the polymer **chains orientation axis** are different. Shear band packets propagate at 38° from the compression axis. **Diffuse shear zone** propagates ahead of the shear band at 45° .

A- Conclusions

Hot Stretching

Polymer chains in hot stretched samples follow the external draw ratio for low extensions. Chain slippage is observed for high extensions. Chain deformations are affine locally but non-affine over large chain portions. SANS results are consistent with birefringence data.

Injection Molding

Chains are better oriented close to the injection gate and close to the sample surface. Mold temperature, injection pressure and cooling time affect chain orientation.

Shear Band Formation

Macromolecules participating in the shear band are oriented at $38^\circ + 45^\circ = 83^\circ$ from the compression axis. Plastic (glide) modes of deformation dominate over diffusive modes.

A- References

B. Hammouda, R.A. Bubeck and D.F.R. Mildner, “Macromolecular Orientation in Hot Stretched and Injection Molded Polystyrene”, *Polymer* 27, 393-397 (1986)

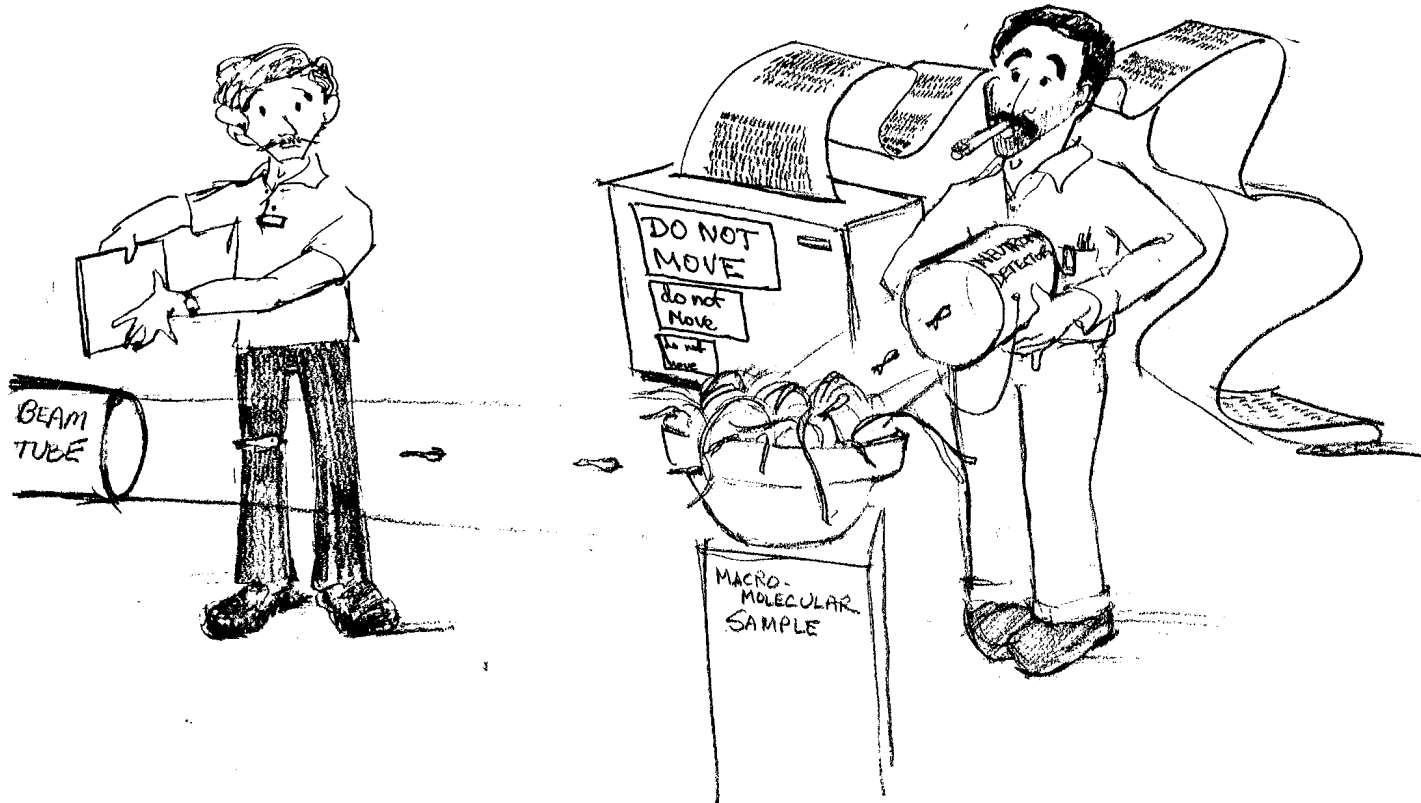
R.A. Bubeck, B. Hammouda and H. Kaiser, “Macromolecular Orientation Associated with Shear bands in Compressed Polystyrene”, *Polymer Communications* 27, 354-356 (1986)

B. Hammouda, D.F.R. Mildner, R.A. Bubeck and M.T. Malanga, “The Inclination Angle of Nonisotropic Inhomogeneties Determined by SANS”, *J. Appl. Cryst.* 19, 320-323 (1986)

J Healey, G.H. Edward and R.B. Knott, “Residual Orientation in Injection-Molded Samples”, *Physica B* 385-386, 620-622 (2006)

30-years ago!

LET THE NEUTS OUT!



B- SANS RESOLUTION AND NEUTRON FOCUSING

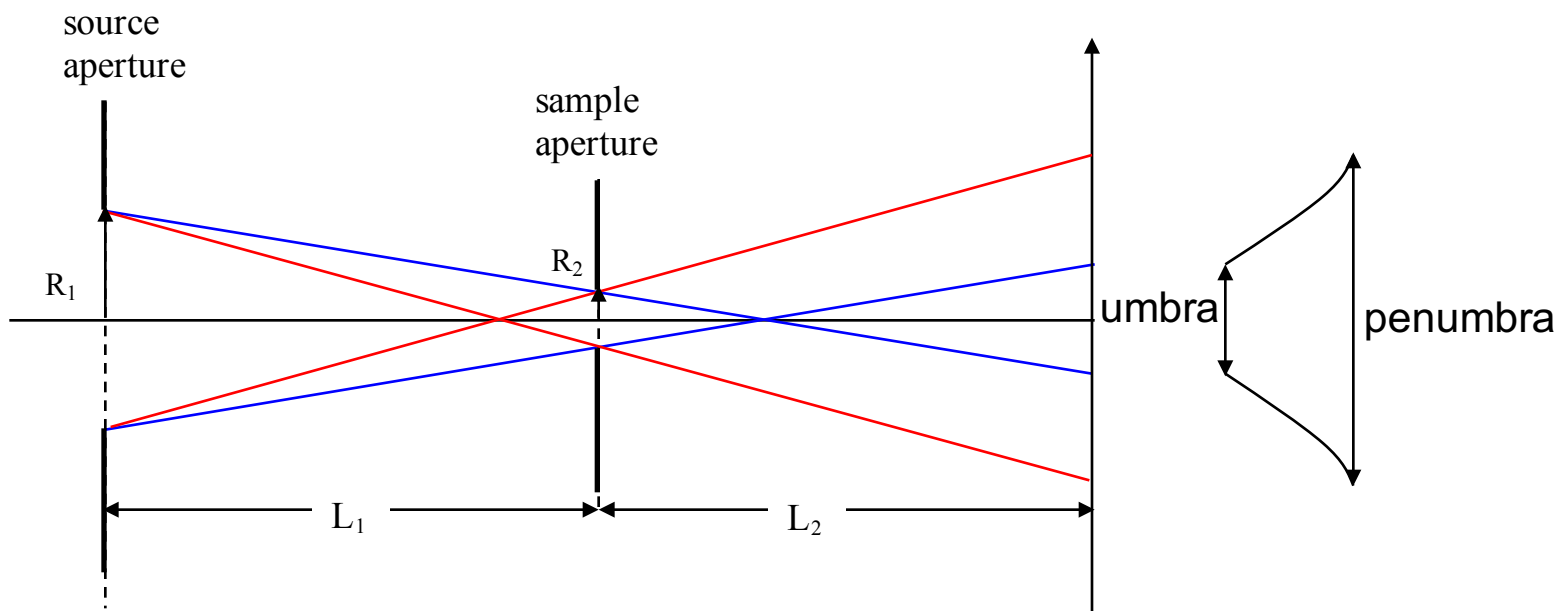
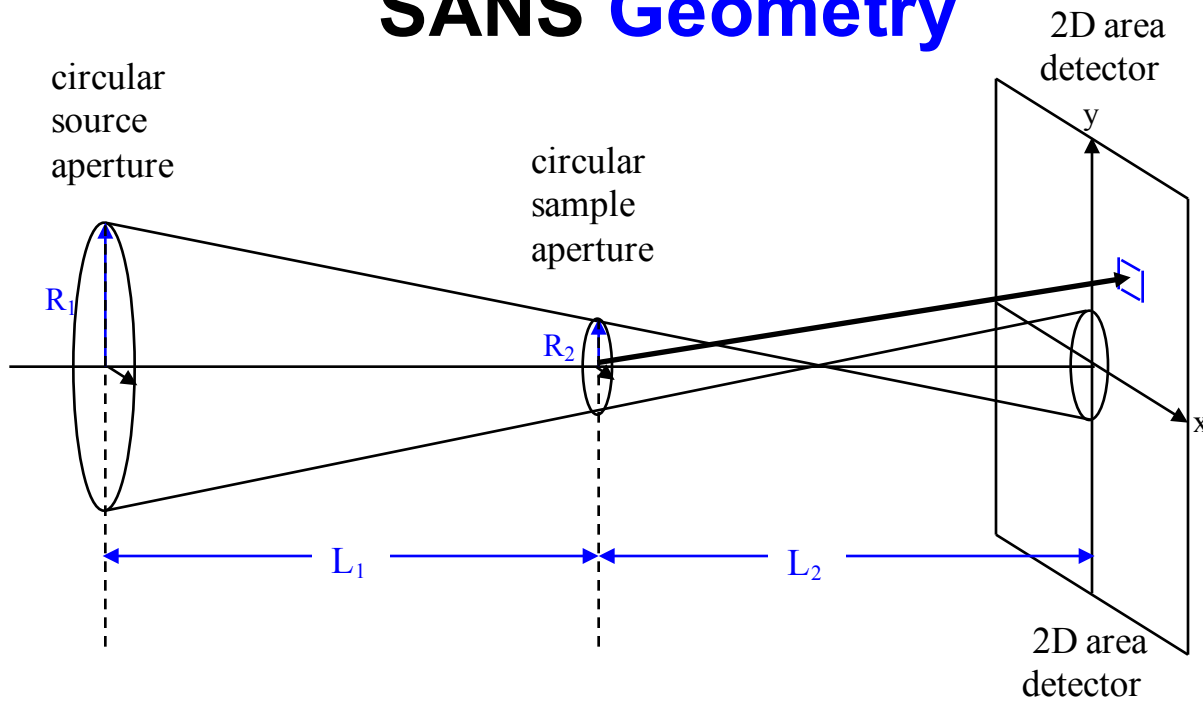
- 1. Components of the Q Resolution Variance
- 2. SANS Resolution with Focusing Lenses
- 3. The Out-of-Focus and the Off-Axis Beam Conditions
- 4. Neutron Focusing Tests
- 5. Ray-Tracing McStas Monte Carlo Simulations

1. Components of the Q Variance

Contributions to the Variance of the SANS resolution σ_Q^2

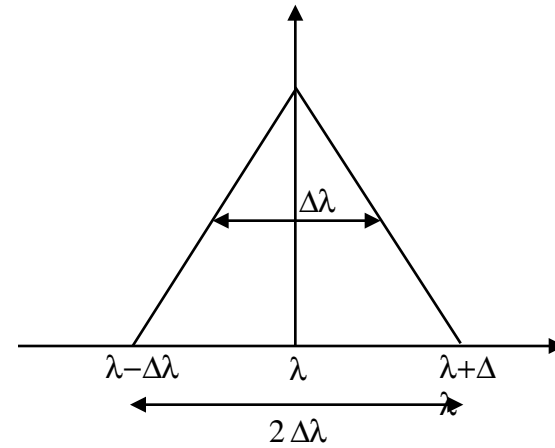
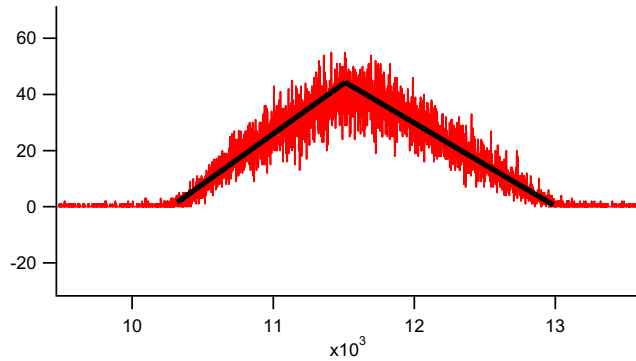
- SANS Geometry
- Wavelength Spread
- Gravity Effect

SANS Geometry

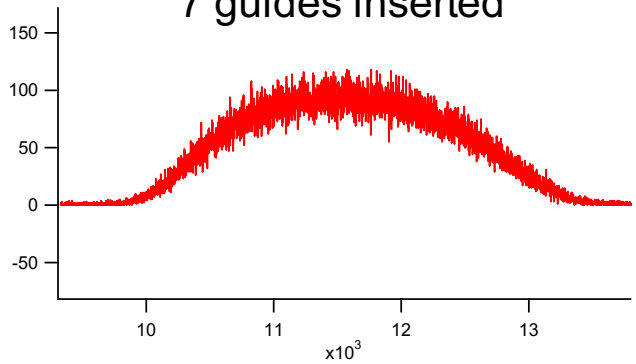


Neutron Wavelength Spread

1 guide inserted

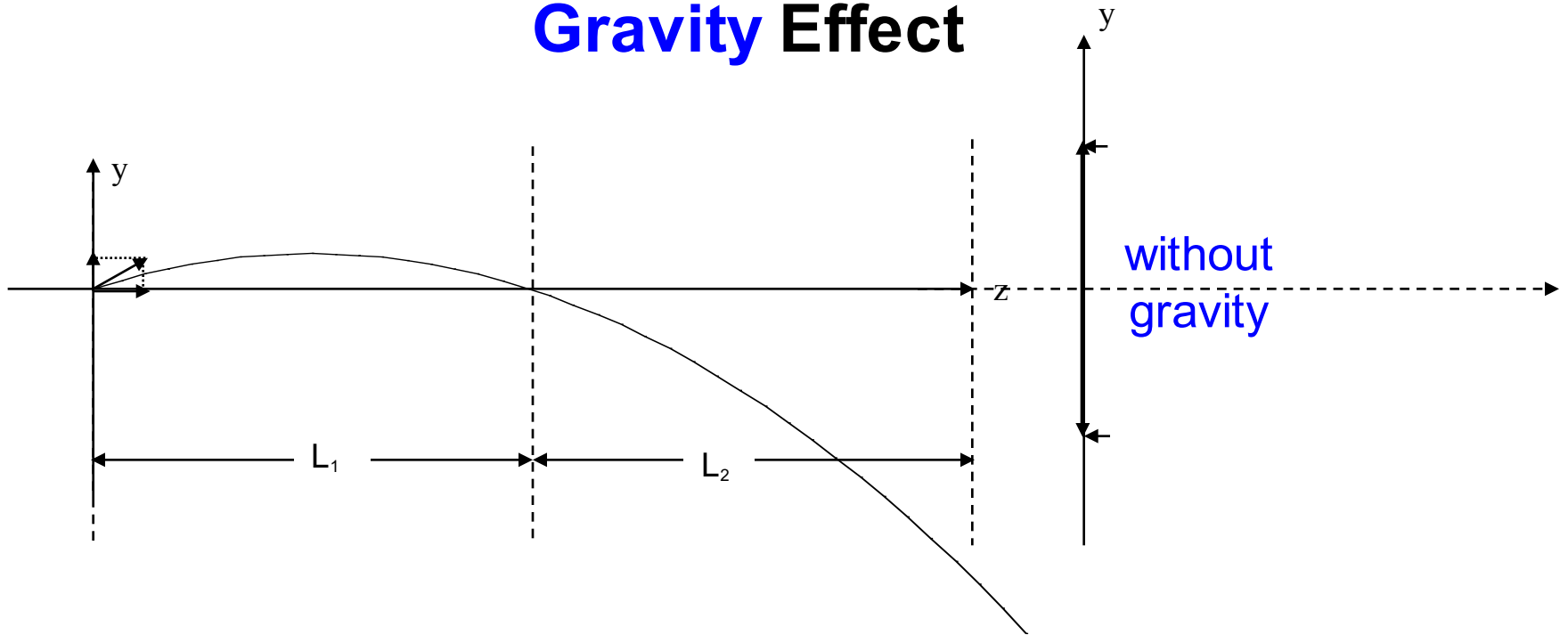


7 guides inserted



Flight Time

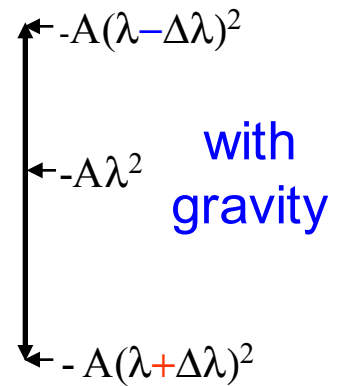
Gravity Effect



Parabola: $y = y_0 - A\lambda^2$

$$A = L_2(L_1 + L_2) \frac{gm^2}{2h^2}$$

Oval contours



Variance of the Q-Resolution σ_Q^2

Geometry

Wavelength
Spread

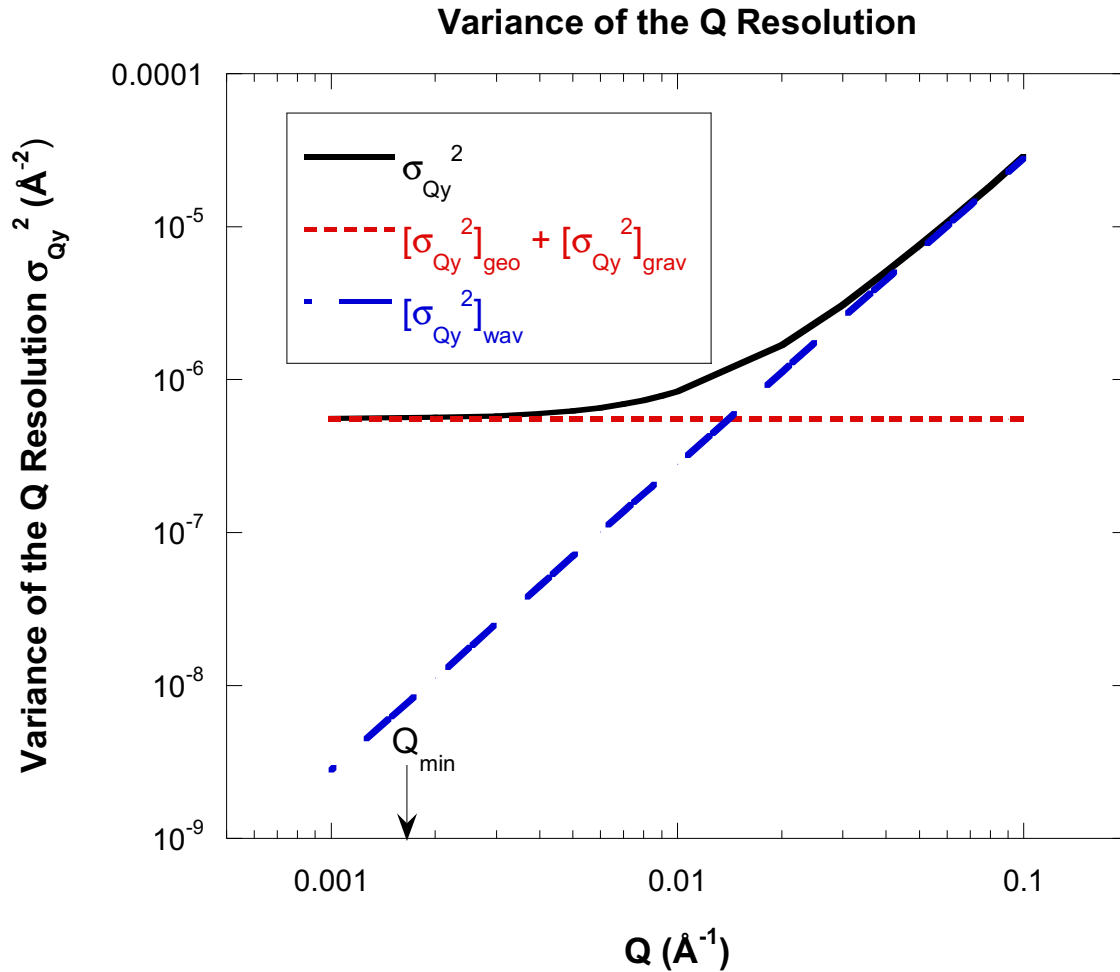
$$\sigma_{Q_x}^2 = \left(\frac{2\pi}{\lambda L_2}\right)^2 \left[\left(\frac{L_2}{L_1}\right)^2 \frac{R_1^2}{4} + \left(\frac{L_1+L_2}{L_1}\right)^2 \frac{R_2^2}{4} + \frac{1}{3} \left(\frac{\Delta x_3}{2}\right)^2 \right] + Q_x^2 \frac{1}{6} \left(\frac{\Delta\lambda}{\lambda}\right)^2$$

$$\sigma_{Q_y}^2 = \left(\frac{2\pi}{\lambda L_2}\right)^2 \left[\left(\frac{L_2}{L_1}\right)^2 \frac{R_1^2}{4} + \left(\frac{L_1+L_2}{L_1}\right)^2 \frac{R_2^2}{4} + \frac{1}{3} \left(\frac{\Delta y_3}{2}\right)^2 \right] + A^2 \lambda^4 \frac{2}{3} \left(\frac{\Delta\lambda}{\lambda}\right)^2 + Q_y^2 \frac{1}{6} \left(\frac{\Delta\lambda}{\lambda}\right)^2$$

$$A = L_2(L_1 + L_2) \frac{gm^2}{2h^2}$$

Gravity Effect

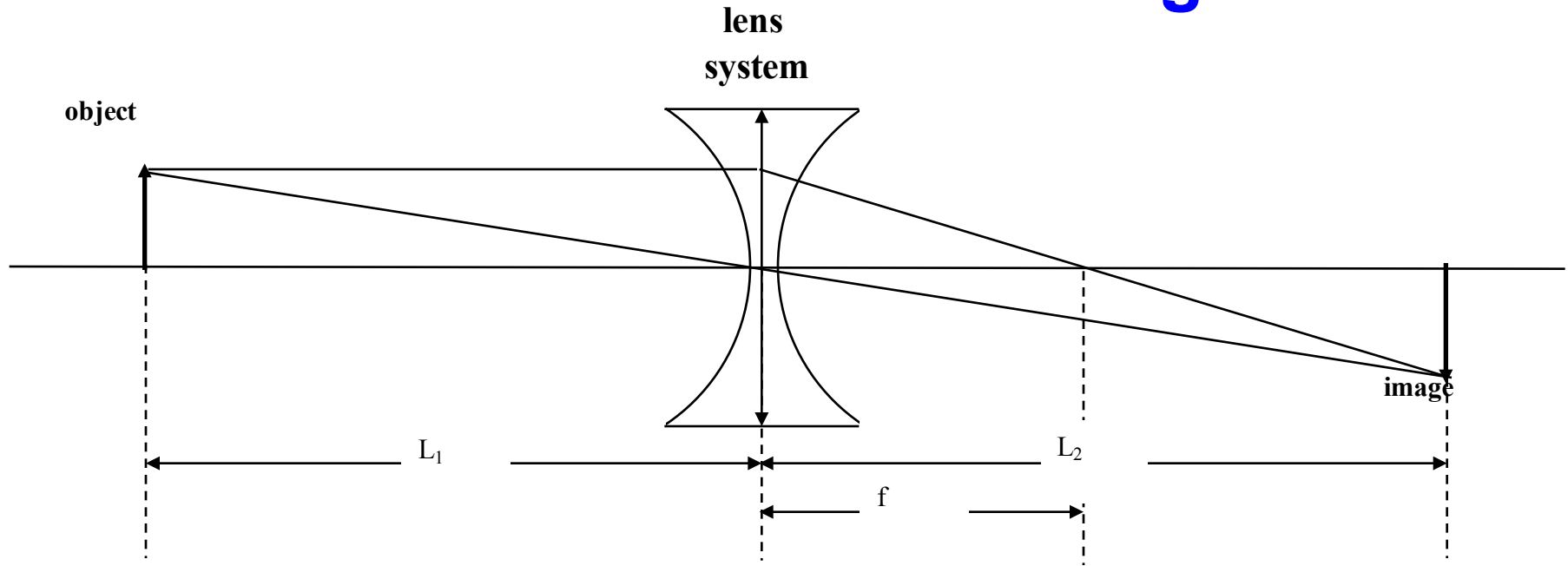
Variance of the Q-Resolution σ_Q^2



$L_1 = 16.14$ m, $L_2 = 13.19$ m, $R_1 = 0.715$ cm, $R_2 = 0.635$ cm
 $\Delta x_3 = \Delta y_3 = 0.5$ cm, $\lambda = 6 \text{\AA}$, $\Delta\lambda/\lambda = 0.13$.

2. SANS Resolution with Focusing Lenses

SANS Resolution with **Focusing Lenses**



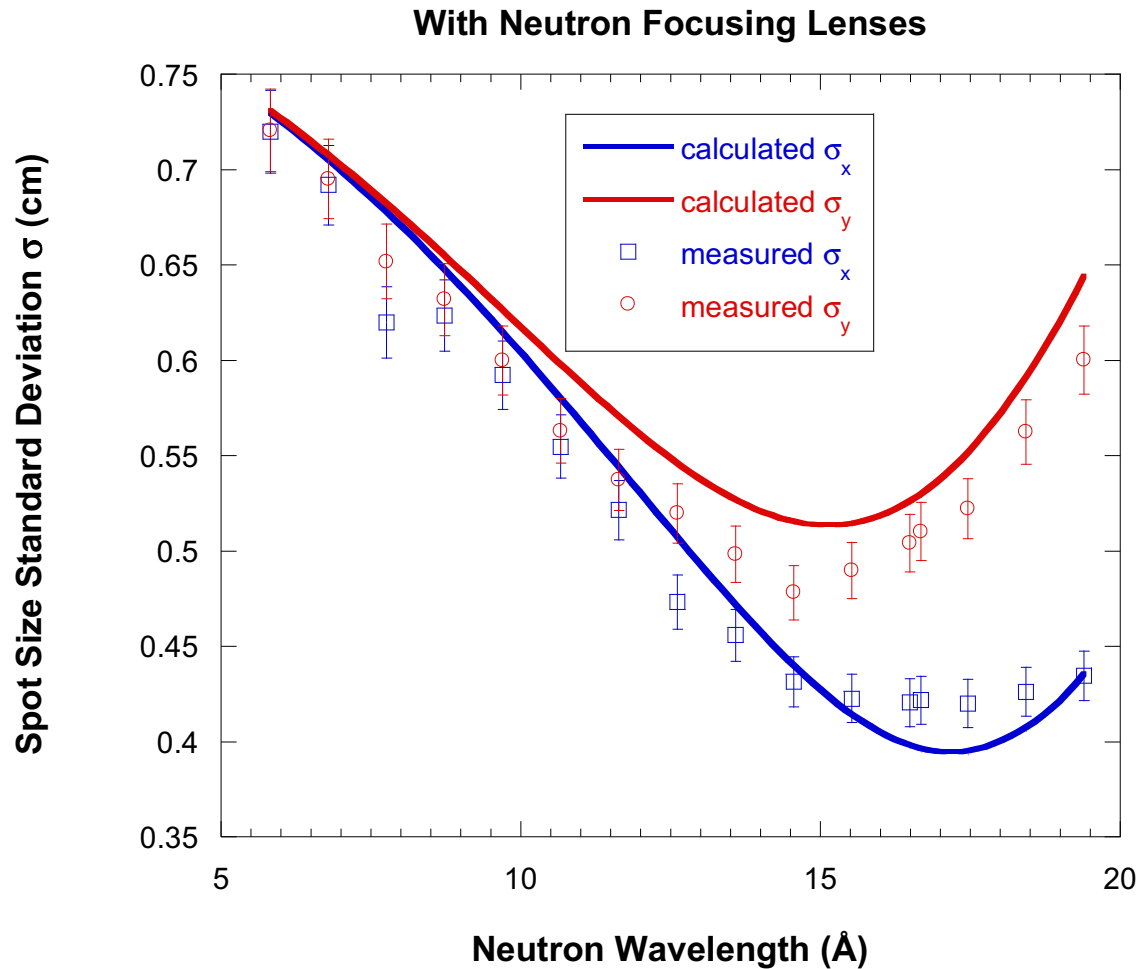
Without Lenses

$$\sigma_{Q_x}^2 = \left(\frac{2\pi}{\lambda L_2} \right)^2 \left[\left(\frac{L_2}{L_1} \right)^2 \frac{R_1^2}{4} + \left(\frac{L_1 + L_2}{L_1} \right)^2 \frac{R_2^2}{4} + \frac{1}{3} \left(\frac{\Delta x_3}{2} \right)^2 \right] + Q_x^2 \frac{1}{6} \left(\frac{\Delta \lambda}{\lambda} \right)^2$$

With Lenses

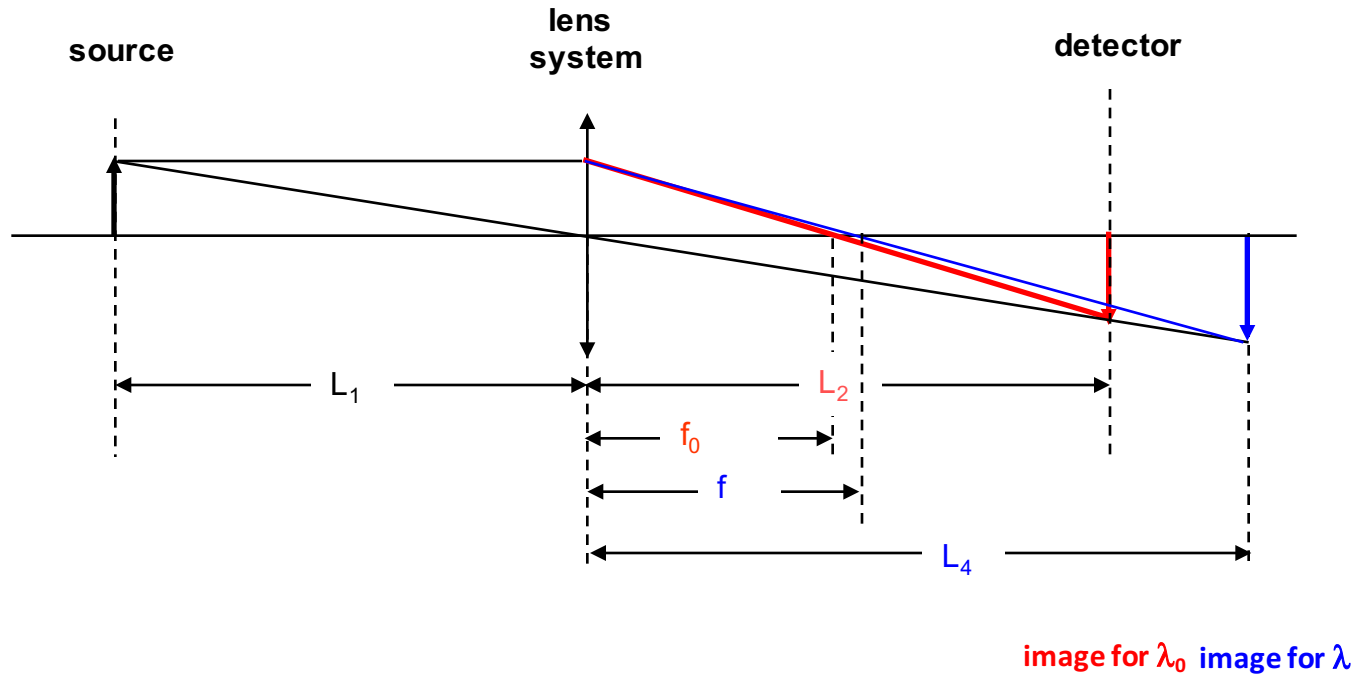
$$\sigma_{Q_x}^2 = \left(\frac{2\pi}{\lambda L_2} \right)^2 \left[\left(\frac{L_2}{L_1} \right)^2 \frac{R_1^2}{4} + \left(\frac{L_1 + L_2}{L_1} \right)^2 \frac{2}{3} \left(\frac{\Delta \lambda}{\lambda} \right)^2 \frac{R_2^2}{4} + \frac{1}{3} \left(\frac{\Delta x_3}{2} \right)^2 \right] + Q_x^2 \frac{1}{6} \left(\frac{\Delta \lambda}{\lambda} \right)^2$$

Variance of the SANS Resolution with Neutron Focusing Lenses



3. The Out-of-Focus and the Off-Axis Beam Conditions

The Out-of-Focus Condition



Optics for the out-of-focus condition

The Out-of-Focus Condition

Variance of the Q-Resolution σ_Q^2

$$\sigma_{Q_x}^2 = \left(\frac{2\pi}{\lambda L_2} \right)^2 \left[\left(\frac{L_2}{L_1} \right)^2 \frac{R_1^2}{4} + \left(\frac{L_1 + L_2}{L_1} \right)^2 S(\lambda, \lambda_0) \frac{R_2^2}{4} + \frac{1}{3} \left(\frac{\Delta x_3}{2} \right)^2 \right] + Q_x^2 \frac{1}{6} \left(\frac{\Delta \lambda}{\lambda} \right)^2$$

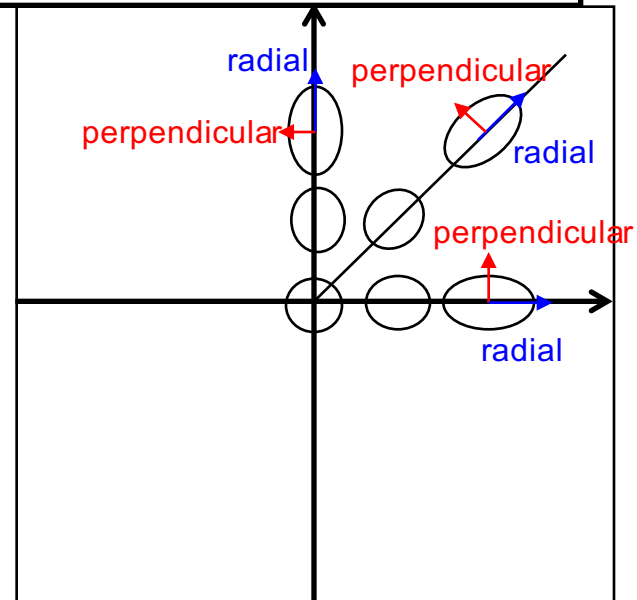
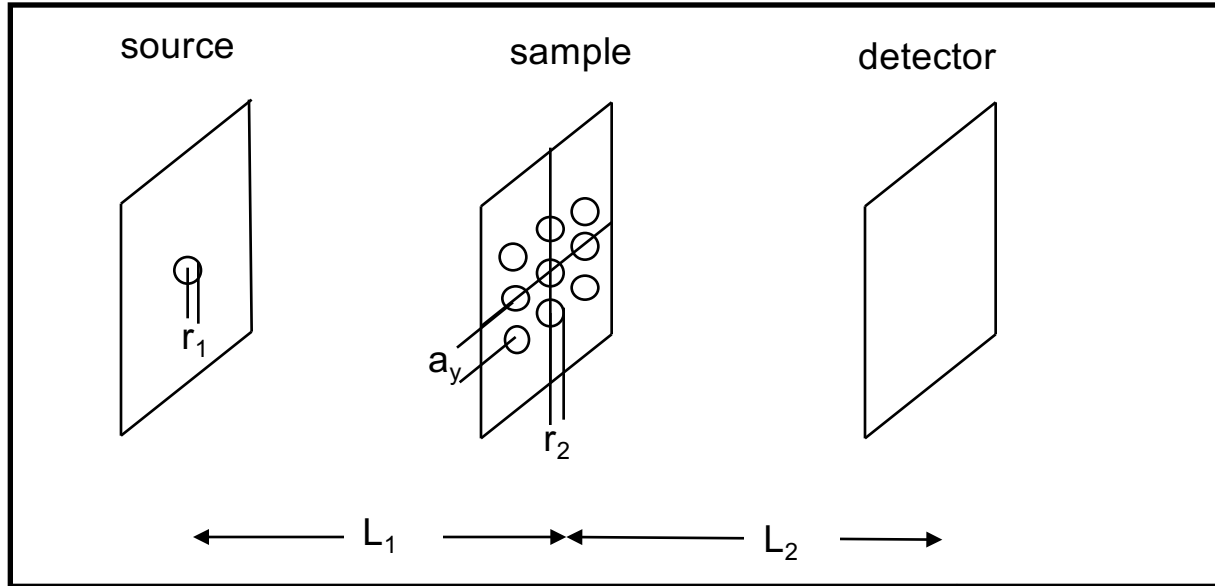
$$S(\lambda, \lambda_0) = \left(1 - \left\{ \frac{\lambda}{\lambda_0} \right\}^2 \right)^2 + \left(\frac{\Delta \lambda}{\lambda} \right)^2 \left(\frac{\lambda}{\lambda_0} \right)^2 \left[\left(\frac{\lambda}{\lambda_0} \right)^2 - \frac{1}{3} \right] + \frac{1}{15} \left(\frac{\lambda}{\lambda_0} \right)^4 \left(\frac{\Delta \lambda}{\lambda} \right)^4$$

Limits:

$$S(\lambda, \lambda_0 \rightarrow \infty) = 1 \quad \text{no lenses}$$

$$S(\lambda \rightarrow \lambda_0) = \frac{2}{3} \left(\frac{\Delta \lambda}{\lambda} \right)^2 = 4 \left(\frac{\sigma_\lambda}{\lambda} \right)^2 \quad \text{in-focus condition} \quad \sigma_\lambda^2 = (1/6)\Delta\lambda^2$$

The Off-Axis Beam Condition



The Off-Axis Beam Condition

new off-axis term

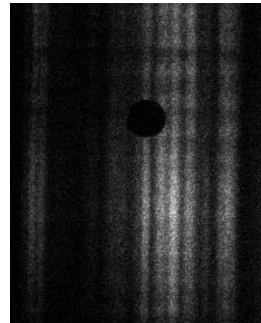
$$\sigma_{xr}^2 = \left[\sigma_x^2 \right]_{\text{geo}} + \left[2n_x a_x \left(1 + \frac{L_2}{L_1} \right) \left(\frac{\lambda}{\lambda_0} \right)^2 \right]^2 \left(\frac{\sigma_\lambda}{\lambda} \right)^2$$

and $\lambda_0 = \sqrt{\frac{1}{N} \left(\frac{\pi}{\rho b} \right) R \frac{L_1 + L_2}{L_1 L_2}}$

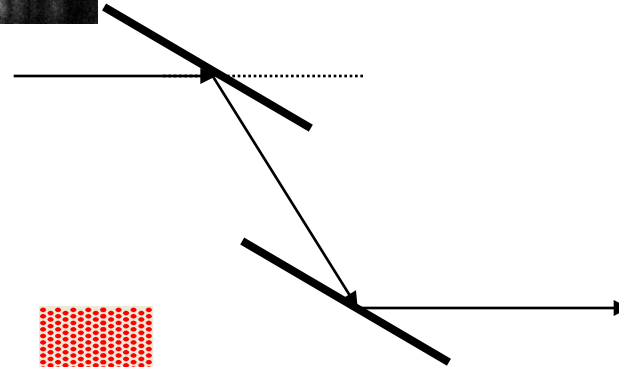
4. Neutron Focusing Tests

The VSANS Instrument at Saclay

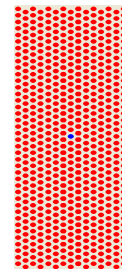
- Stripped neutron beam



- Double crystal monochromator



- 13 masks with 600 holes each



- Image plate neutron detector with 0.15 mm resolution – MAR 345

The **VSANS** Instrument Configuration

Instrument geometry:

$$L_1 = 3730 \text{ mm}, r_1 = 0.64 \text{ mm},$$

$$L_2 = 6078 \text{ mm}, r_2 = 0.45 \text{ mm}, a_2 = 2.24 \text{ mm}$$

$$\Delta x_3 = 0.15 \text{ mm}$$

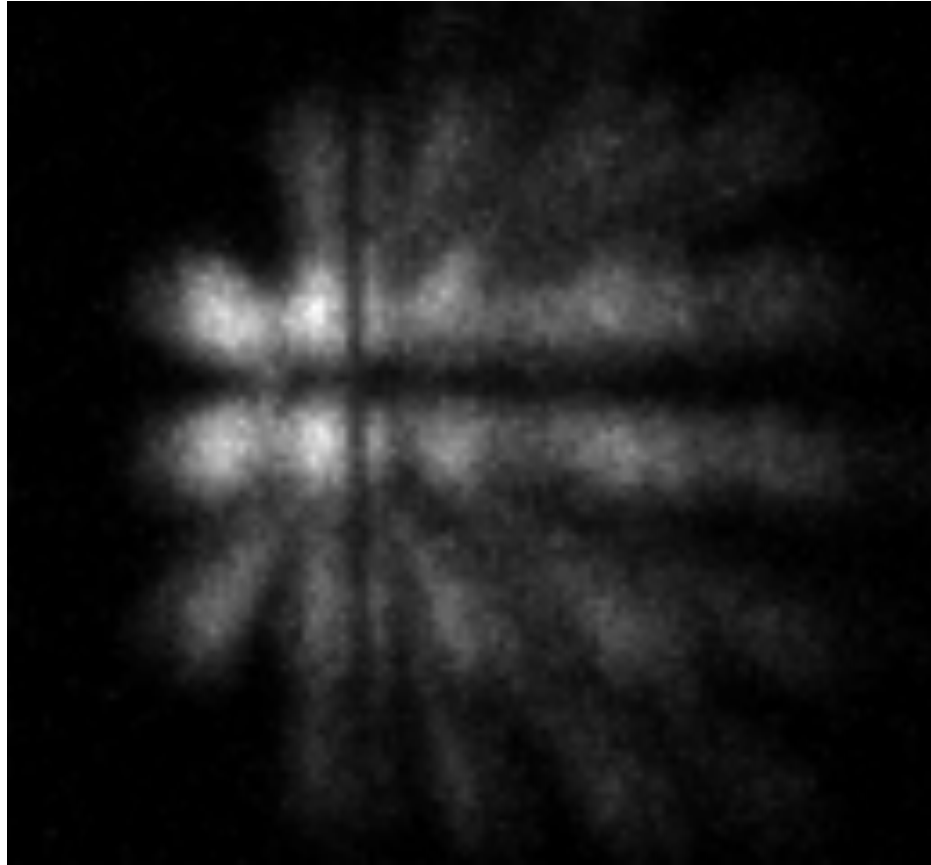
Discrete neutron wavelengths:

$$\lambda = 6 \text{ \AA}, 9.1 \text{ \AA}, 12.34 \text{ \AA} \text{ or } 14.59 \text{ \AA}$$

Wavelength spread:

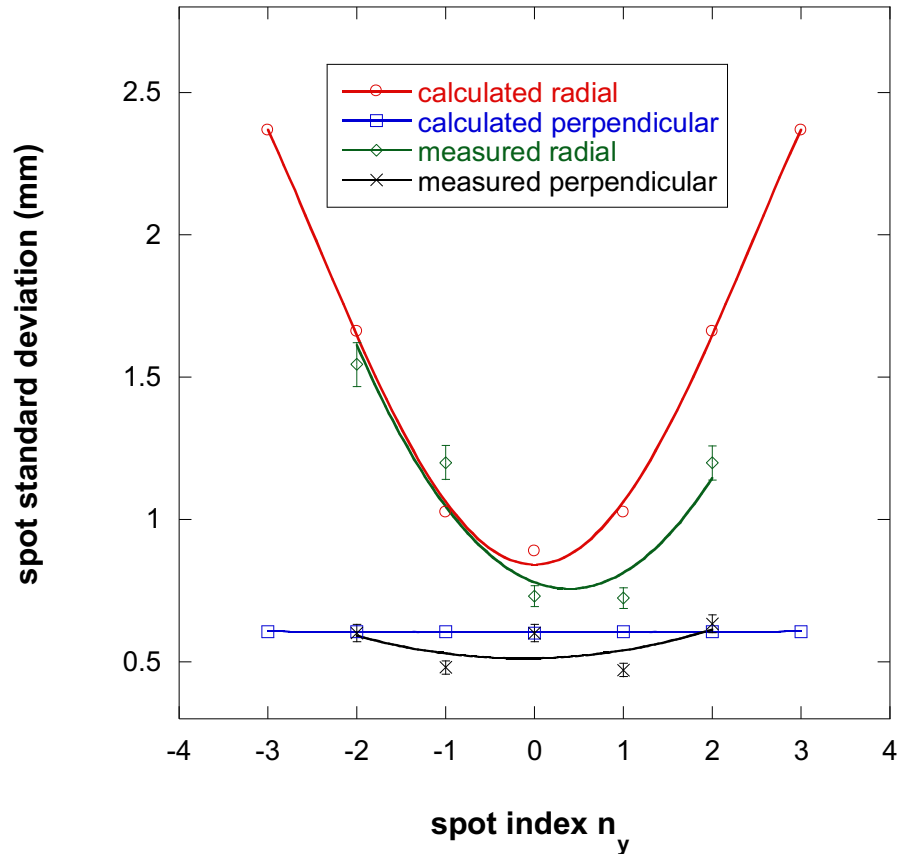
$$\frac{\Delta\lambda}{\lambda} = 0.15$$

Neutron Focusing Tests



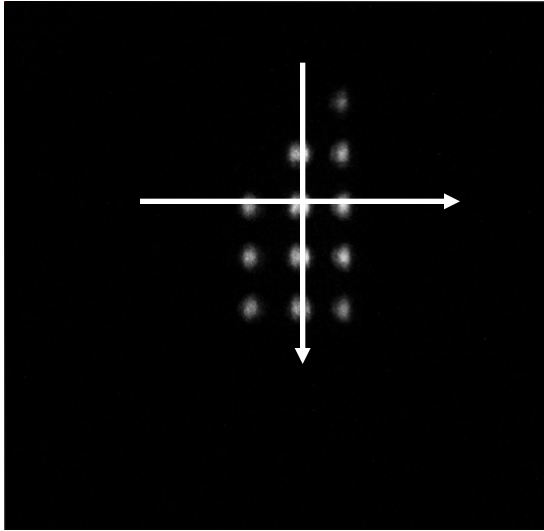
Neutron focusing test performed using $N = 30$ lenses and a neutron wavelength $\lambda = 12.34 \text{ \AA}$.

Spot Standard Deviations

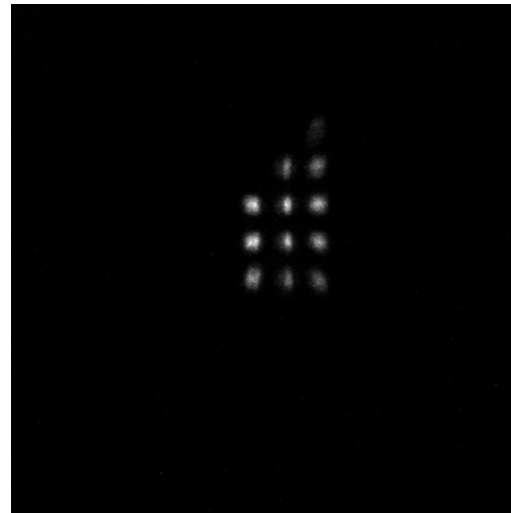


Neutron focusing test performed using $N = 30$ lenses and a neutron wavelength $\lambda = 12.34 \text{ \AA}$. Comparison of the calculated and measured standard deviations of the spot variances in the radial and perpendicular directions for the vertical series of spots (varying n_y).

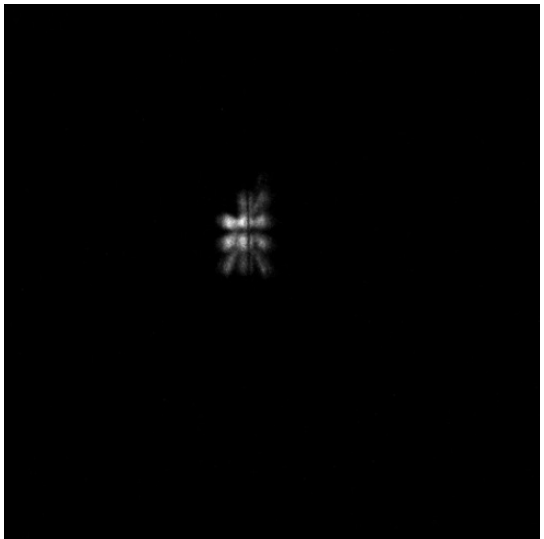
Spots on the Detector



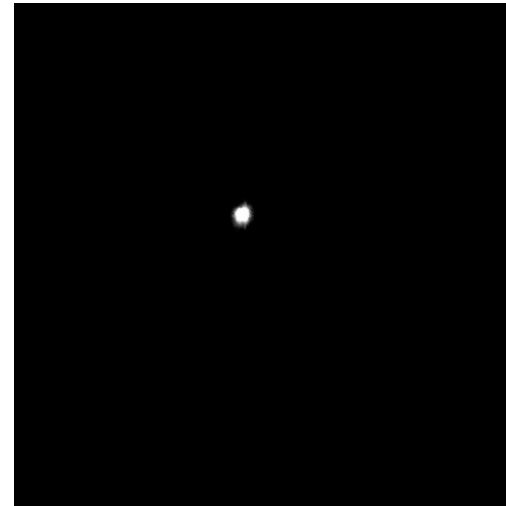
$$\lambda = 6 \text{ \AA}$$



$$\lambda = 9.1 \text{ \AA}$$



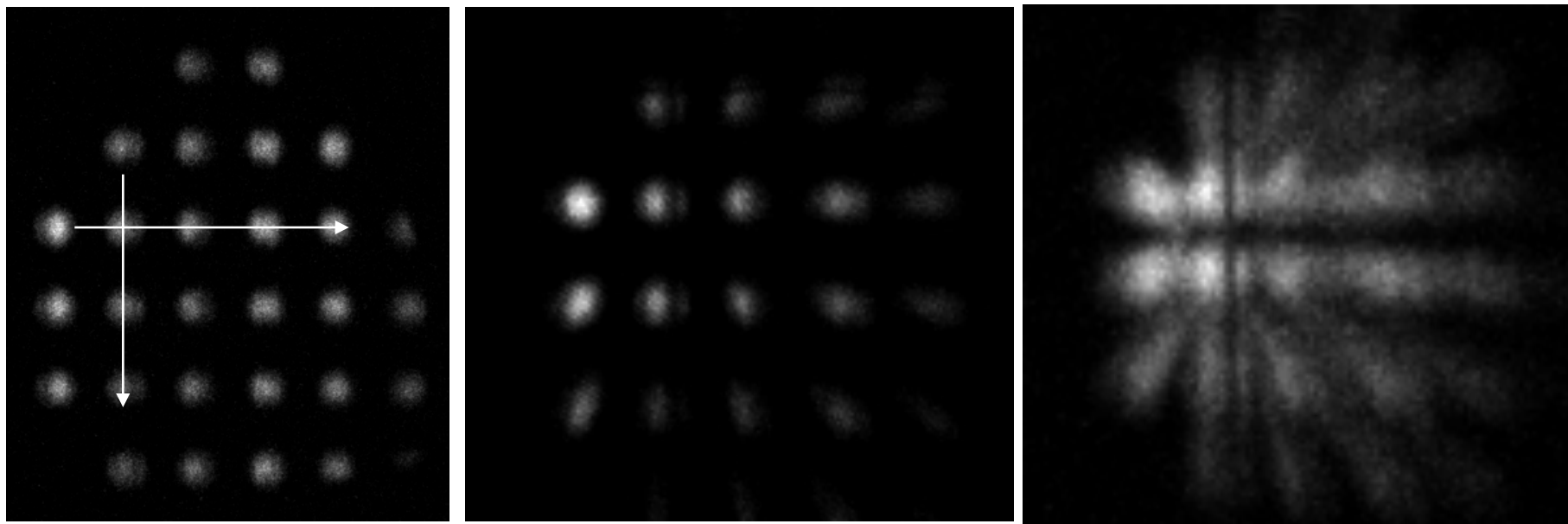
$$\lambda = 12.34 \text{ \AA}$$



$$\lambda = 14.59 \text{ \AA}$$

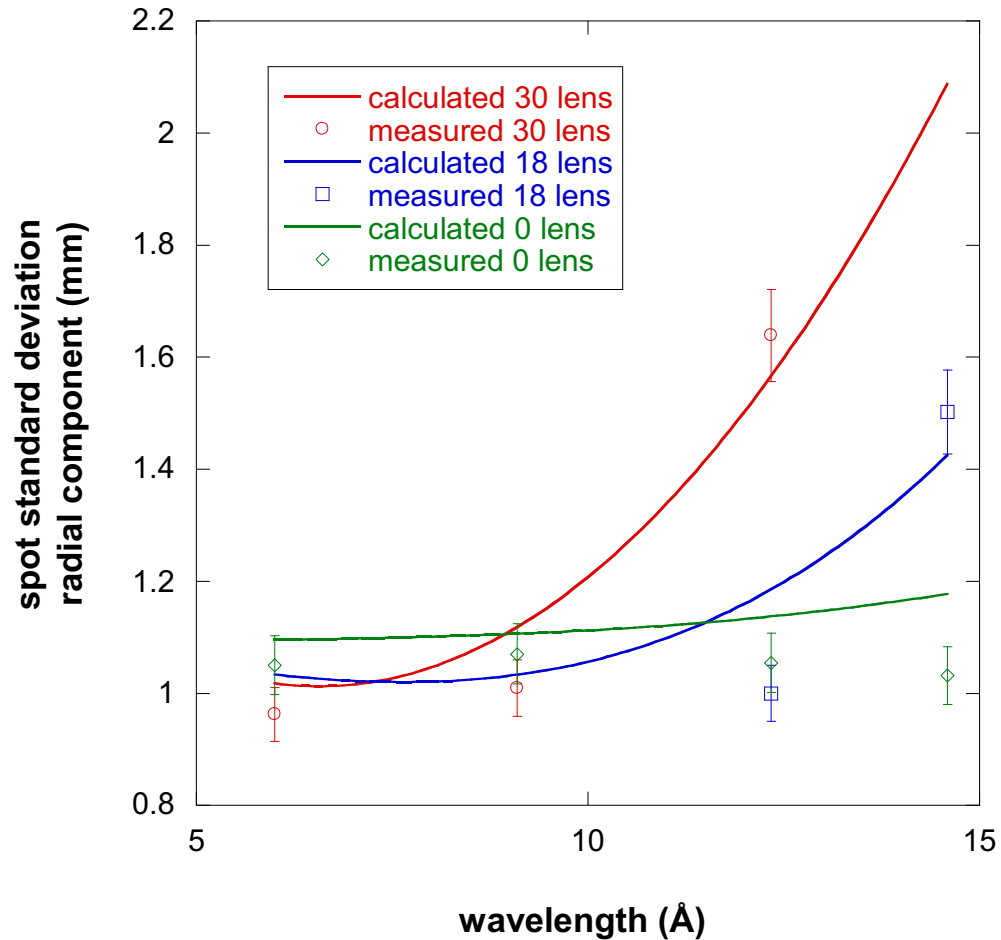
Neutron spots when 30 lenses are used. Changing wavelength focuses the various spots and distorts them along the radial direction.

Spots on the Detector



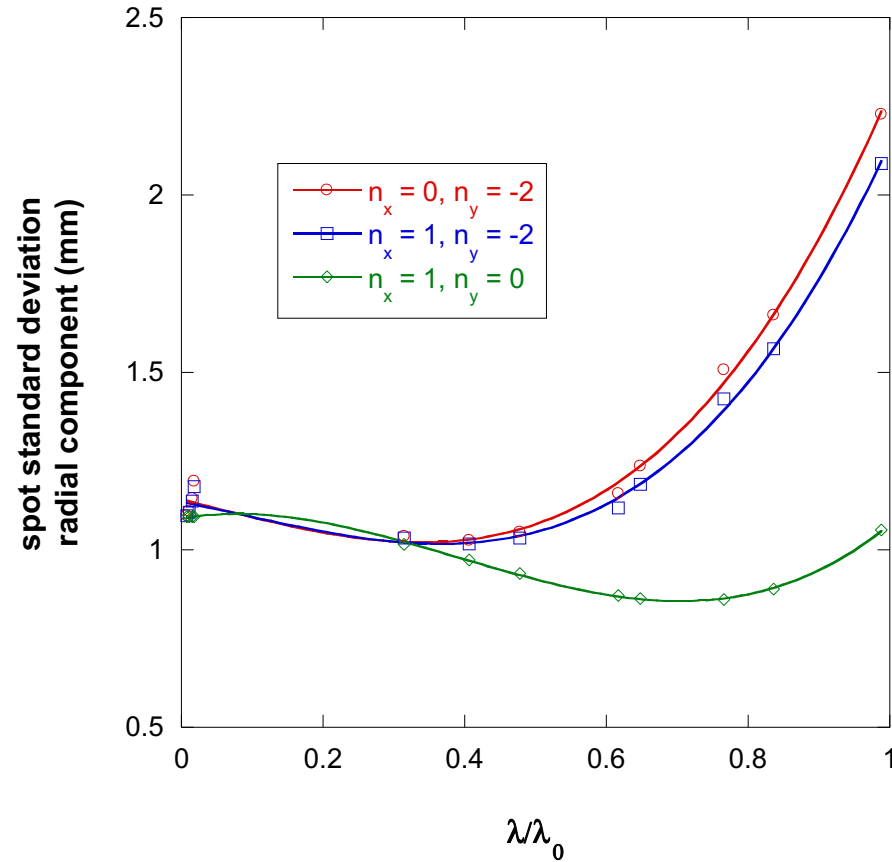
Neutron spots for a neutron wavelength of 12.34 \AA and varying the number of lenses $N = 0$ (left), $N = 18$ (center) and $N = 30$ (right).

Spots Standard Deviations



Variation of the calculated and measured standard deviations in the radial direction for one of the spots (with indices $n_x = 1$ and $n_y = -2$) for increasing neutron wavelength and changing the number of lenses.

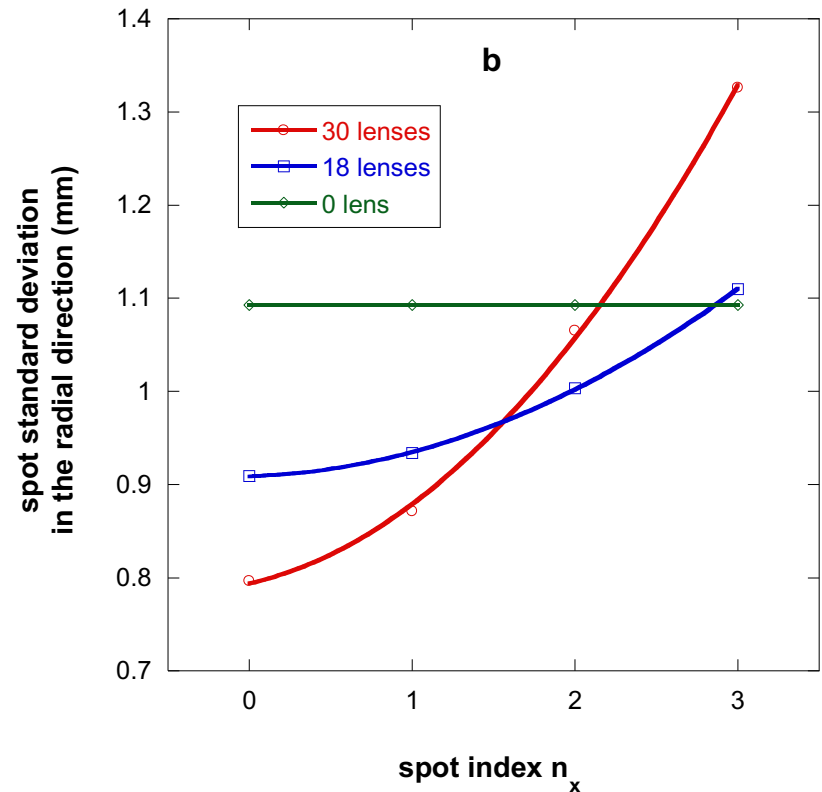
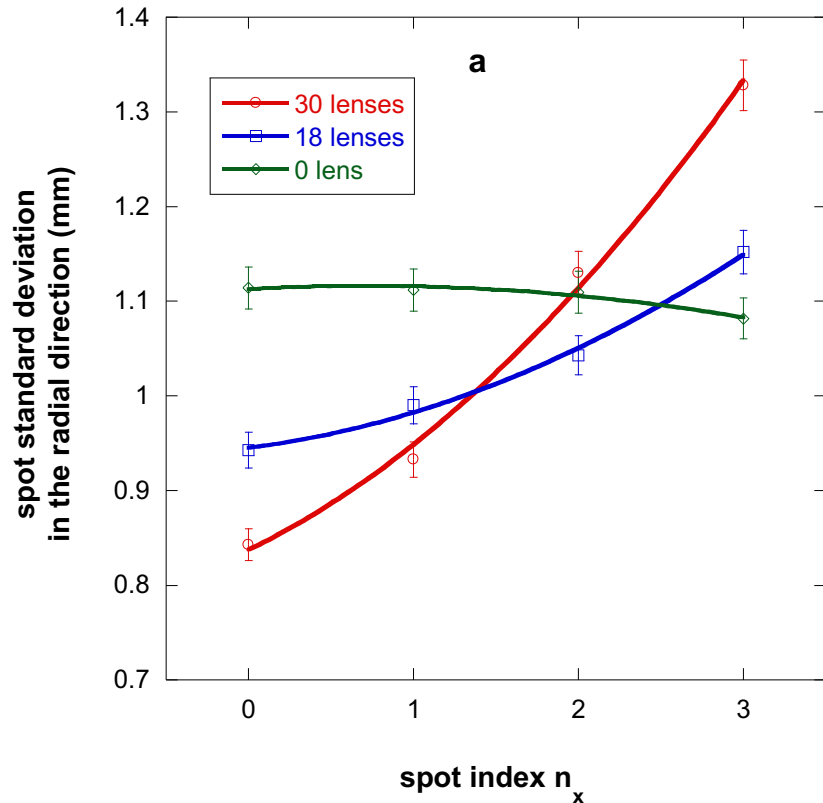
Spots Standard Deviations



Variation of the neutron beam spot standard deviation (radial component) with varying λ/λ_0 for three different off-axis neutron beams. λ is the neutron wavelength and λ_0 is the focusing wavelength for N lenses. ($\lambda_0=14.76$ Å for N=30, $\lambda_0=19.05$ Å for N=18 and λ_0 = large for N=0)

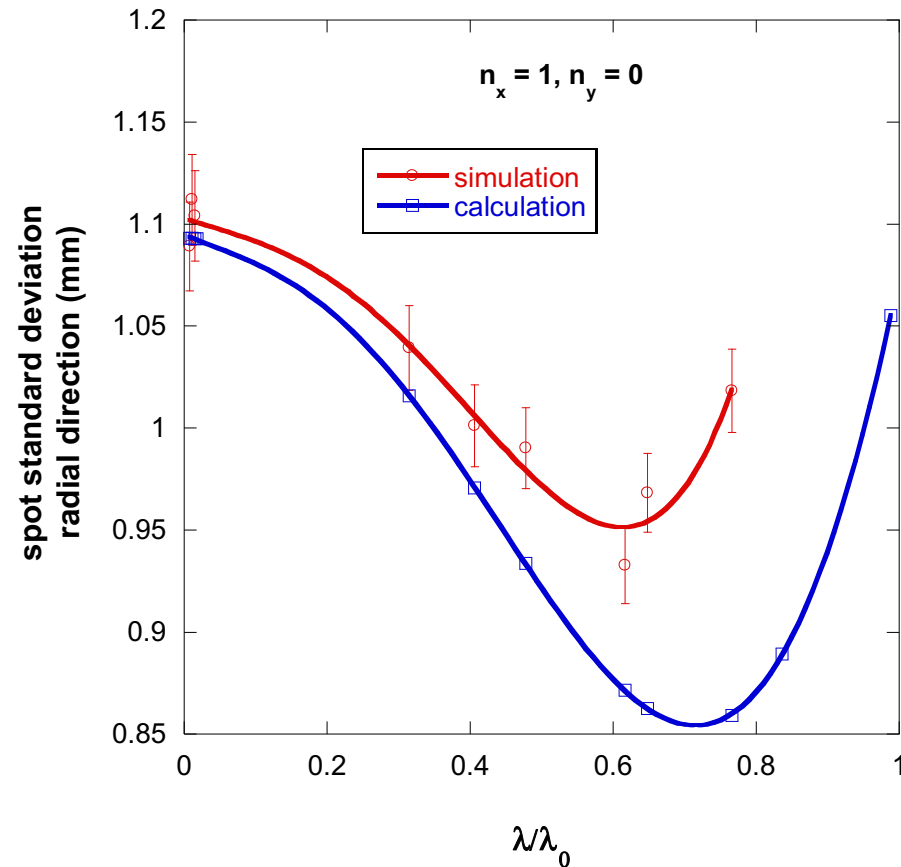
5. Ray-Tracing McStas Simulation

Spots Standard Deviations



Simulation results on the left (a) and analytical results on the right (b) representing the standard deviation of the beam spot profile in the radial direction for the main (on-axis) beam and three off-axis beams for 9.1 \AA wavelength. The three cases of 30 lenses, 18 lenses and no lens are plotted.

Spots Standard Deviations



Comparison of the simulation and analytical calculation approaches plotted with increasing dimensionless parameter λ/λ_0 for spot ($n_x=1, n_y=0$)

B- References

- D.F.R. Mildner and J.M. Carpenter, "Optimization of the Experimental Resolution for SAS", *J. Appl. Cryst.* 17, 249-256 (1984).
- B. Hammouda and D.F.R. Mildner, "SANS Resolution with Refractive Optics", *J. Appl. Cryst.* 40, 250-259 (2007).
- B. Hammouda, D.F.R. Mildner, A. Brulet and S. Desert, "Insight into Neutron Focusing – the Out-of-focus Condition", *J. Appl. Cryst.* 46, 1361-1371 (2013).